INTERNATIONAL JOURNAL FOR NUMERICAL AND ANALYTICAL METHODS IN GEOMECHANICS
Int. J. Numer. Anal. Meth. Geomech., **23**, 1559–1578 (1999)

WAVE–INDUCED PORE PRESSURE AROUND A BURIED PIPELINE IN GIBSON SOIL: FINITE ELEMENT ANALYSIS

D. S. JENG[1,*] AND Y. S. LIN[2]

[1]*School of Engineering, Gold Coast Campus, Griffith University, QLD 9726, Australia*
[2]*Department of Civil Engineering, National Chung-Hsing University, Taichung 40227, Taiwan, R.O.C.*

SUMMARY

The water wave–induced pore pressure on a pipeline buried in a porous seabed is investigated. Unlike conventional investigations, shear modulus of the seabed is considered to vary with soil depth in this study. The boundary value problem describing soil stresses as well as pore water pressure under periodical wave loading is solved numerically by using a Finite Element Method. Employing the principle of repeatability, the lateral boundary conditions are obtained first and verified with previous analytical solutions. Then, the wave–sealed–pipe interaction problem can be solved to obtain the wave–induced soil response. The effects of variable shear modulus, geometry of the pipe and the degree of saturation on the wave–induced pore pressure are found to be significant. Copyright © 1999 John Wiley & Sons, Ltd.

KEY WORDS: pore pressure; seabed response; Gibson soil; pipeline; waves

1. INTRODUCTION

Recently, considerable efforts have been dedicated to the phenomenon of the wave–seabed–structure interaction. One reason for the growing interests of this problem is that many offshore installations (such as breakwaters, pipelines, platform, etc.) have been reported to be damaged by the wave-induced seabed response in the vicinity of structures,[1–3] rather than from constructional causes. Another reason is that poro-elastic theories for the wave–soil interaction problem have been further applied to the field measurements, such as the determination of the shear modulus of soils[4] and the directional spectra of ocean surface waves,[5] as well as acoustic waves propagating through porous media.[6]

A marine pipeline is a type of common — used offshore installations. It has been widely used for disposal and municipal waste water into the sea, for cooling water in nuclear power plants and so on. Design of marine pipelines with regarding to their stability is a rather complicated problem. In general, the fluctuations of wave pressures at the surface of the seabed induce excess pore pressures and effective stresses. When the pore pressure becomes excessive with accompanying decrease in effective stress, a sedimentary bed may be moved in either horizontal (liquefaction) or vertical directions (shear failure), then lead to an instability of the seabed.[7–10] Thus, one of the

*Correspondence to: D.-S. Jeng, School of Engineering, Gold Coast Campus, Griffith University, PMB 50 Gold Coast Mail Centre, QLD 9726, Australia. E-mail: d.jeng@mailbox.gu.edu.au

Contract/grant sponsor: Australian Research Council
Contract/grant sponsor: National Science Council in Taiwan

CCC 0363–9061/99/131559–20$17.50

Received March 1998
Revised 15 June 1998

dominant factors that must be taken into considerations in the analysis of stability of the pipeline is the wave-induced seabed response around the pipelines.

Two significant mechanisms of the wave-induced soil response have been observed in laboratory experiments and field measurements.[11,12] The first is resulted from the transient or oscillatory excess pore pressure, and is accompanied by damping of the amplitude and phase lag in change of the pore pressure. This type of soil response appears in response to the periodic fluctuations in each wave.[13,14] The important factor of this mechanism is the degree of saturation. The second is the residual or progressive nature of the pore pressure, which appears at the initial stage of cyclic loading. This type of soil response is caused by the build-up of excess pore pressure due to cyclic loading, much as can happen during a seismic event.[15–17] In this study, only the wave-induced oscillatory soil response will be investigated.

Shear modulus of the seabed is one of important factors that affect the wave-induced seabed response. However, most previous investigations for water–soil–pipe interaction in the literature have so far assumed the modulus of soil as uniform through the soil matrix. In fact, the rigidity of soil generally increases with soil depth as a consequence of increasing effective overburden pressure in natural seabeds. For a consolidation problem, the medium whose modulus increases linearly with soil depth (which is so-called Gibson soil) has been studied in the past.[18] Furthermore, some evidence for the modulus of soils varying with depth has been reported in the literature.[19,20]

Numerous theories have been developed for the wave-induced soil response in an elastic seabed in the past, based on different assumptions of the rigidity of the soil skeleton and compressibility of pore fluid. Among these, Yamamoto *et al.*[13] and Madsen[14] have proposed analytical solutions for the water waves–soil interaction problem within a uniform seabed of infinite thickness, respectively. This framework has been extended to a seabed of finite thickness,[21] as well as a layered seabed,[22] through a semi-analytical method. Later, Mei and Foda[23] proposed a boundary-layer approximation for the wave-induced soil response. The approximation has been limited to a seabed of fine sand. It has been found to lose accuracy in coarse sand.[24] Later, Jeng and Seymour[25] proposed an exact solution for the wave-induced soil response in a seabed with variable permeability. They concluded that variable permeability significantly affects the soil response. The first author has attempted to derive an analytical solution for the wave-induced soil response in Gibson soil, but not successful.

Besides the development of analytical solutions, numerical simulations have been widely applied to examine the wave-seabed interaction problem in recent years, such as a finite difference method,[12,26] a finite element method[27–32] and a boundary element method.[33] However, all aforementioned investigations have only examined the soil response in a poro-elastic seabed under the action of two-dimensional progressive waves, without the presence of a marine structure. Recently, a series of analytical solutions for the wave-induced soil response in the vicinity of a vertical reflected wall has been developed systematically by the first author.[34–37] However, all these investigations have only concerned with the wave-induced soil response in the vicinity of a breakwater.

Although the importance of wave–soil–pipeline interaction phenomenon has been addressed in the literature,[3] this problem has not been fully understood because of the complicated soil behaviour and geometry of the pipeline. Based on a potential theory, the hydrodynamic uplift forces on the buried pipelines have been studied.[38–40] However, the potential theory is far away from the realistic conditions of the soil and pore-fluid two-phase medium. Furthermore, the potential theory provides no information for the effective stresses and soil displacements in the seabed, which have been recognized as dominant factors in the analysis of seabed instability.

Based on Biot's model,[41,42] the wave-induced pore pressure around a buried pipeline has been studied through a boundary integral equation method[43] and a finite element method.[44,45] Among these, Cheng and Liu[43] considered a buried pipe in a region that are surrounded by two impermeable walls. Magda[44,45] considered a similar case with a wider range of the degree of saturation. All these have only considered a uniform porous seabed. To date, it seems that the mechanisms of the wave-induced pore pressure in a porous seabed with variable shear modulus (for example, Gibson soil) have not been explored.

In this paper, a finite element model will be proposed to investigate the wave-induced seabed response around a buried pipeline in Gibson soil. To obtain the lateral boundary conditions, the wave-induced soil response in a seabed without a pipeline will be solved numerically, employing the principle of repeatability. The soil response with a buried pipeline can then be obtained. Based on the proposed numerical model, the influences of variable shear modulus, geometry of the pipe and the degree of saturation on the wave-induced pore pressure will be examined.

2. BOUNDARY VALUE PROBLEM

2.1. Governing equations

Considering a soil column in a porous seabed of finite thickness, a fully buried pipe (with a radius R) is located in the seabed (see Figure 1). The wave crests are assumed to propagate in the positive x-direction, while the z-direction is measured positive upward from impermeable rigid bottom, as shown in Figure 1.

In this study, the problem is modelled by a poro-elastic theory. The consolidation equation,[41,42] extending from Terzaghi's theory, is generally accepted as the governing equation for flow of a compressible pore fluid in a compressible porous medium. For a two-dimensional wave–seabed–pipe interaction problem and treating the porous bed as hydraulically isotropic with the same permeability (K) in all directions, this equation can be expressed as

$$\frac{K}{\gamma_w}\left(\frac{\partial^2 p}{\partial x^2}+\frac{\partial^2 p}{\partial z^2}\right)-n'\beta\frac{\partial p}{\partial t}=-\frac{\partial \varepsilon}{\partial t} \tag{1}$$

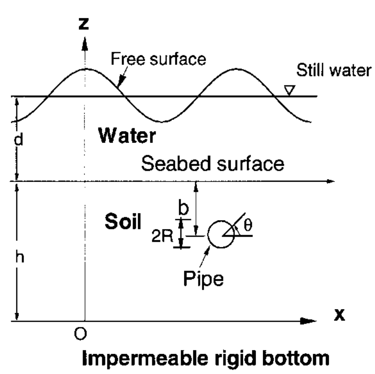

Figure 1. Definition sketch of pipeline buried in seabed

where γ_w is the unit weight of pore water (N/m^3), n' is soil porosity, p is pore pressure (N/m^2), t is the time (s). In equation (1), the compressibility of pore fluid (β) and volumetric strain of soil matrix (ε) are defined by

$$\beta = \frac{1}{K_w} + \frac{1-S}{P_{wo}} \tag{2}$$

$$\varepsilon = \frac{\partial u}{\partial x} + \frac{\partial w}{\partial z} \tag{3}$$

where K_w is the true modulus of elasticity of water (taken as 2×10^9 N/m^2), P_{wo} is the absolute water pressure, S is the degree of saturation and u and w are the soil displacements in the x- and z-directions, respectively.

Under conditions of plane strain, the incremental effective stresses can be expressed as

$$\sigma'_x = 2G(z)\left[\frac{\partial u}{\partial x} + \frac{\mu}{1-2\mu}\,\varepsilon\right] \tag{4}$$

$$\sigma'_x = 2G(z)\left[\frac{\partial w}{\partial z} + \frac{\mu}{1-2\mu}\,\varepsilon\right] \tag{5}$$

$$\tau_{xz} = G(z)\left[\frac{\partial u}{\partial z} + \frac{\partial w}{\partial x}\right] = \tau_{zx} \tag{6}$$

where the shear stresses are expressed in double subscripts, τ_{xz}, denoting the stress in the z-direction on a plane perpendicular to the x-axis. It is noted that a positive sign is taken for a compressive normal stress in this study. The shear modulus of the soil (G) is related to Young's modulus (E) and Poisson's ratio (μ) as $E/2(1+\mu)$. It is worthwhile to point out that the shear modulus (G) in equations (4)–(6) is assumed to be a function of soil depth (z).

Neglecting the effects of body forces and inertia terms, the equations governing the overall equilibrium of a porous medium can be expressed as

$$\frac{\partial \sigma'_x}{\partial x} + \frac{\partial \tau_{xz}}{\partial z} = -\frac{\partial p}{\partial x} \tag{7}$$

$$\frac{\partial \tau_{xz}}{\partial x} + \frac{\partial \sigma'_z}{\partial z} = -\frac{\partial p}{\partial z} \tag{8}$$

in the x- and z-directions, respectively.

Substituting equations (4)–(6) into equations (7) and (8), the equation of motion can be written as

$$G(z)\nabla^2 u + \frac{G(z)}{1-2\mu}\frac{\partial \varepsilon}{\partial x} + \frac{\mathrm{d}G(z)}{\mathrm{d}z}\left[\frac{\partial u}{\partial z} + \frac{\partial w}{\partial x}\right] = -\frac{\partial p}{\partial x} \tag{9}$$

$$G(z)\nabla^2 w + \frac{G(z)}{1-2\mu}\frac{\partial \varepsilon}{\partial z} + \frac{2}{1-2\mu}\frac{\mathrm{d}G(z)}{\mathrm{d}z}\left[\mu\frac{\partial u}{\partial x} + (1-\mu)\frac{\partial w}{\partial z}\right] = -\frac{\partial p}{\partial z} \tag{10}$$

2.2. Boundary conditions

For a porous seabed of finite thickness, as shown in Figure 1, the evaluation of the wave-induced seabed response requires the solution of (1), (9) and (10), together with the appropriate boundary conditions.

(a) *Bottom Boundary Conditions* (*BBC*): Firstly, zero displacements and no vertical flow occur at the impermeable horizontal bottom, i.e.

$$u = w = \frac{\partial p}{\partial z} = 0 \quad \text{at } z = 0 \tag{11}$$

(b) *Boundary Conditions at Seabed Surface* (*SBC*): Secondly, we assume that the bottom frictional stress is small and negligible. The vertical effective normal stress and shear stress vanish and pore pressure is equal to the wave pressure at the surface of the seabed, i.e.

$$\begin{aligned} \sigma'_z &= \tau_{xz} = 0 \\ p &= \frac{\gamma_w H}{2\cosh kd}\cos(kx - \omega t) \quad \text{at } z = h \\ &= p_o \,\mathrm{Re}\left\{(\cos kx + \mathrm{i}\sin kx)\mathrm{e}^{-\mathrm{i}\omega t}\right\} \end{aligned} \tag{12}$$

where p_o denotes the amplitude of the wave pressure at the surface of the seabed, d is water depth, H is wave height, k is the wave number and ω is the wave frequency. In equation (12), Re represents the real part of function in the brackets.

(c) *Boundary conditions along the Pipe Surface* (*PBC*): Thirdly, it is reasonable to assume that there is no flow through the pipeline wall. Thus, the pressure gradient on the surface of the pipe ($r = R$) should vanish, i.e.

$$\frac{\partial p}{\partial n} = 0 \quad \text{at } r = \sqrt{(x - x_o)^2 + (z - z_o)^2} = R \tag{13}$$

where x_o and z_o denote the co-ordination of the centre of the pipe and n is the normal direction to the surface of the pipeline.

(d) *Lateral Boundary Conditions* (*LBC*): Finally, since the existence of the pipeline only affects the wave-induced soil response in the vicinity of the pipe, the 'disturbed pressure' from the pipeline should vanish at points far away from the pipe. However, the seabeds at points are still under wave loading. Thus, the lateral boundary conditions at these points are given by the solution without pipeline, which will be described later.

It is noted that the lateral boundary conditions used here are different from those of Magda.[44,45] He assumed that the soil displacements and the gradient of pore pressure vanished at points far away from the pipe. This implies that the soil response will vanish at these points under wave loading. However, it is clear that the wave-induced soil displacements and the gradient of pore pressure are not zero because the seabed is under wave loading. Thus, a more reasonable assumption is that the effect of the pipe vanishes at points far away from the pipe, but the soil response owing to wave loading still exists.

3. FINITE ELEMENT ANALYSIS

3.1. Finite element formations

Since the wave-induced oscillatory soil response is periodically fluctuating in the temporal domain, the wave-induced pore pressure, effective stresses and soil displacements can be expressed as

$$\begin{bmatrix} p(x,z;t) \\ u(x,z;t) \\ w(x,z;t) \\ \sigma'_x(x,z;t) \\ \sigma'_z(x,z;t) \\ \tau_{xz}(x,z;t) \end{bmatrix} = \left(\begin{bmatrix} P_{\mathrm{r}}(x,z;t) \\ U_{\mathrm{r}}(x,z;t) \\ W_{\mathrm{r}}(x,z;t) \\ S_{x\mathrm{r}}(x,z;t) \\ S_{z\mathrm{r}}(x,z;t) \\ T_{xz\mathrm{r}}(x,z;t) \end{bmatrix} + \mathrm{i} \begin{bmatrix} P_{\mathrm{c}}(x,z;t) \\ U_{\mathrm{c}}(x,z;t) \\ W_{\mathrm{c}}(x,z;t) \\ S_{x\mathrm{c}}(x,z;t) \\ S_{z\mathrm{c}}(x,z;t) \\ T_{xz\mathrm{c}}(x,z;t) \end{bmatrix} \right) \mathrm{e}^{-\mathrm{i}\omega t} \tag{14}$$

where subscripts 'r' and 'c' represent the real and imaginary parts of the soil response, respectively.

Substituting (14) into equation (1), and then directly applying the Galerkin method,[46] to these equations, the finite element analytical formulations can be written as

$$\begin{aligned} \int_S N_i \begin{Bmatrix} q_{n\mathrm{r}} \\ q_{n\mathrm{c}} \end{Bmatrix} \mathrm{d}S &= \int_S N_i \frac{K}{\gamma_w} \left[\begin{Bmatrix} \dfrac{\partial P_{\mathrm{r}}}{\partial x} \\ \dfrac{\partial P_{\mathrm{c}}}{\partial x} \end{Bmatrix} n_x + \begin{Bmatrix} \dfrac{\partial P_{\mathrm{r}}}{\partial z} \\ \dfrac{\partial P_{\mathrm{c}}}{\partial z} \end{Bmatrix} n_z \right] \mathrm{d}S \\ &= \int_V \frac{\partial N_i}{\partial x} \frac{K}{\gamma_w} \begin{Bmatrix} \dfrac{\partial P_{\mathrm{r}}}{\partial x} \\ \dfrac{\partial P_{\mathrm{c}}}{\partial x} \end{Bmatrix} \mathrm{d}V + \int_V \frac{\partial N_i}{\partial z} \frac{K}{\gamma_w} \begin{Bmatrix} \dfrac{\partial P_{\mathrm{r}}}{\partial z} \\ \dfrac{\partial P_{\mathrm{c}}}{\partial z} \end{Bmatrix} \mathrm{d}V + \int_V N_i \omega \begin{Bmatrix} -\dfrac{\partial U_{\mathrm{c}}}{\partial x} \\ \dfrac{\partial U_{\mathrm{r}}}{\partial x} \end{Bmatrix} \mathrm{d}V \\ &\quad + \int_V N_i \omega \begin{Bmatrix} -\dfrac{\partial W_{\mathrm{c}}}{\partial z} \\ \dfrac{\partial W_{\mathrm{r}}}{\partial z} \end{Bmatrix} \mathrm{d}V - \int_V N_i n' \beta \omega \begin{Bmatrix} -P_{\mathrm{c}} \\ P_{\mathrm{r}} \end{Bmatrix} \mathrm{d}V \end{aligned} \tag{15}$$

where N_i represents the shape function of the ith node.

Introducing (14) into (9), the finite element form is given as

$$\begin{aligned} &\int_V N_i \frac{2G(z)(1-\mu)}{1-2\mu} \begin{Bmatrix} \dfrac{\partial^2 U_{\mathrm{r}}}{\partial x^2} \\ \dfrac{\partial^2 U_{\mathrm{c}}}{\partial x^2} \end{Bmatrix} \mathrm{d}V + \int_V N_i G(z) \begin{Bmatrix} \dfrac{\partial^2 U_{\mathrm{r}}}{\partial z^2} \\ \dfrac{\partial^2 U_{\mathrm{c}}}{\partial z^2} \end{Bmatrix} \mathrm{d}V + \int_V N_i \frac{G(z)}{1-2\mu} \begin{Bmatrix} \dfrac{\partial^2 W_{\mathrm{r}}}{\partial x \partial z} \\ \dfrac{\partial^2 W_{\mathrm{c}}}{\partial x \partial z} \end{Bmatrix} \mathrm{d}V \\ &\quad + \int_V N_i \frac{\mathrm{d}G(z)}{\mathrm{d}z} \begin{Bmatrix} \dfrac{\partial U_{\mathrm{r}}}{\partial z} \\ \dfrac{\partial U_{\mathrm{c}}}{\partial z} \end{Bmatrix} \mathrm{d}V + \int_V N_i \frac{\mathrm{d}G(z)}{\mathrm{d}z} \begin{Bmatrix} \dfrac{\partial W_{\mathrm{r}}}{\partial x} \\ \dfrac{\partial W_{\mathrm{c}}}{\partial x} \end{Bmatrix} \mathrm{d}V + \int_V N_i \begin{Bmatrix} \dfrac{\partial P_{\mathrm{r}}}{\partial x} \\ \dfrac{\partial P_{\mathrm{c}}}{\partial x} \end{Bmatrix} \mathrm{d}V = 0 \end{aligned} \tag{16}$$

Applying the principle of partial integration to the above equation, after some algebraic manipulation, the equation is rendered as

$$\int_S N_i \begin{Bmatrix} f_{xr} \\ f_{xc} \end{Bmatrix} \mathrm{d}S = \int_S N_i \left(\begin{Bmatrix} S_{xr} \\ S_{xc} \end{Bmatrix} n_x + \begin{Bmatrix} T_{xzr} \\ T_{xzc} \end{Bmatrix} n_z \right) \mathrm{d}S$$

$$= \int_V 2G(z) \frac{\partial N_i}{\partial x} \left[\begin{Bmatrix} \dfrac{\partial U_r}{\partial z} \\ \dfrac{\partial U_c}{\partial z} \end{Bmatrix} + \frac{\mu}{1-2\mu} \left(\begin{Bmatrix} \dfrac{\partial U_r}{\partial x} \\ \dfrac{\partial U_c}{\partial x} \end{Bmatrix} + \begin{Bmatrix} \dfrac{\partial W_r}{\partial z} \\ \dfrac{\partial W_c}{\partial z} \end{Bmatrix} \right) \right] \mathrm{d}V$$

$$+ \int_V \frac{\partial N_i}{\partial z} G(z) \left[\begin{Bmatrix} \dfrac{\partial U_r}{\partial z} \\ \dfrac{\partial U_c}{\partial z} \end{Bmatrix} + \begin{Bmatrix} \dfrac{\partial W_r}{\partial z} \\ \dfrac{\partial W_c}{\partial z} \end{Bmatrix} \right] \mathrm{d}V - \int_V N_i \begin{Bmatrix} \dfrac{\partial P_r}{\partial x} \\ \dfrac{\partial P_c}{\partial x} \end{Bmatrix} \mathrm{d}V \tag{17}$$

Similarly, equation (10) can also be derived in finite element form as

$$\int_S N_i \begin{Bmatrix} f_{zr} \\ f_{zc} \end{Bmatrix} \mathrm{d}S = \int_S N_i \left(\begin{Bmatrix} S_{zr} \\ S_{zc} \end{Bmatrix} n_z + \begin{Bmatrix} T_{xzr} \\ T_{xzc} \end{Bmatrix} n_x \right) \mathrm{d}S$$

$$= \int_V 2G(z) \frac{\partial N_i}{\partial x} \left[\begin{Bmatrix} \dfrac{\partial U_r}{\partial z} \\ \dfrac{\partial U_c}{\partial z} \end{Bmatrix} + \begin{Bmatrix} \dfrac{\partial W_r}{\partial x} \\ \dfrac{\partial W_c}{\partial x} \end{Bmatrix} \right] \mathrm{d}V - \int_V N_i \begin{Bmatrix} \dfrac{\partial P_r}{\partial z} \\ \dfrac{\partial P_c}{\partial z} \end{Bmatrix} \mathrm{d}V$$

$$+ \int_V \frac{\partial N_i}{\partial z} G(z) \left[\begin{Bmatrix} \dfrac{\partial W_r}{\partial z} \\ \dfrac{\partial W_c}{\partial z} \end{Bmatrix} + \frac{\mu}{1-2\mu} \left(\begin{Bmatrix} \dfrac{\partial U_r}{\partial x} \\ \dfrac{\partial U_c}{\partial x} \end{Bmatrix} + \begin{Bmatrix} \dfrac{\partial W_r}{\partial z} \\ \dfrac{\partial W_c}{\partial z} \end{Bmatrix} \right) \right] \mathrm{d}V \tag{18}$$

For an individual element, equation (15) can be expressed in matrix form as

$$\int_S N_I [\mathbf{Q}_e]\, \mathrm{d}S = \int_V \mathbf{B}_1^T \mathbf{D}_1 \mathbf{B}_1 \, \mathrm{d}V [\mathbf{P}] + \int_V \mathbf{B}_2^T \mathbf{D}_2 \mathbf{B}_2 \, \mathrm{d}V [\mathbf{P}] + \int_V \mathbf{B}_2^T \mathbf{D}_3 \mathbf{B}_3 \, \mathrm{d}V [\mathbf{U}] \tag{19}$$

$$[\mathbf{Q}_e] = \begin{bmatrix} (q_{nr})_1 & 0 & \cdots & (q_{nr})_{n_e} & 0 \\ 0 & (q_{nc})_1 & & 0 & (q_{nc})_{n_e} \end{bmatrix} \tag{20}$$

$$[\mathbf{F}_e] = \begin{bmatrix} (f_{xr})_1 & 0 & (f_{zr})_1 & 0 & \cdots & (f_{xr})_{n_e} & 0 & (f_{zr})_{n_e} & 0 \\ 0 & (f_{xc})_1 & 0 & (f_{zc})_1 & & 0 & (f_{xc})_{n_e} & 0 & (f_{zc})_{n_e} \end{bmatrix} \tag{21}$$

$$\left(\begin{Bmatrix} q_{nr} \\ q_{nc} \end{Bmatrix}\right)_i = \left(\frac{K}{\gamma_w}\begin{Bmatrix} \dfrac{\partial P_r}{\partial x} \\ \dfrac{\partial P_c}{\partial x} \end{Bmatrix} n_x + \frac{K}{\gamma_w}\begin{Bmatrix} \dfrac{\partial P_r}{\partial z} \\ \dfrac{\partial P_c}{\partial z} \end{Bmatrix} n_z\right)_i \tag{22}$$

where n_e is the number of nodes per element, and coefficient matrices $\mathbf{B}_i$ and $\mathbf{D}_i$ ($i = 1$–3) are given in the appendix.

Similarly, the finite element formations for individual element in equations (17) and (18), can be expressed in matrix form as

$$\int_S N_i[\mathbf{F}_e]\,\mathrm{d}S = \int_V \mathbf{B}_4^{\mathrm{T}}\mathbf{D}_4\mathbf{B}_4\,\mathrm{d}V[\mathbf{U}] + \int_V \mathbf{B}_5^{\mathrm{T}}\mathrm{B}_1\,\mathrm{d}V[\mathbf{P}] \tag{23}$$

$$[\mathbf{F}_e] = \begin{bmatrix} (f_{xr})_1 & 0 & (f_{zr})_1 & 0 & \cdots & (f_{xr})_{n_e} & 0 & (f_{zr})_{n_e} & 0 \\ 0 & (f_{xc})_1 & 0 & (f_{zc})_1 & & 0 & (f_{xc})_{n_e} & 0 & (f_{zc})_{n_e} \end{bmatrix} \tag{24}$$

$$\left(\begin{Bmatrix} f_{xr} \\ f_{xc} \\ f_{zr} \\ f_{zc} \end{Bmatrix}\right)_i = \left(\begin{Bmatrix} S_{xr} \\ S_{xc} \\ T_{xzr} \\ T_{xzc} \end{Bmatrix} n_x + \begin{Bmatrix} T_{xzr} \\ T_{xzc} \\ S_{zr} \\ S_{zc} \end{Bmatrix} n_z\right)_i \tag{25}$$

in which coefficient matrices $\mathbf{B}_i$ ($i = 4$–6) and D_4 are given in the appendix.

3.2. Principle of repeatability

The symmetry of a structure permits a considerable reduction of analysis costs to be achieved is widely appreciated. However, in numerous cases, a repetition of structural form and loading is present while no axes of symmetry exist. For such situations economies of similar type can be made by use of the principle of repeatability.[47] The seabed under periodical wave loading is one of examples.

Considering a periodical waves propagating over a porous seabed (Figure 2), in which a series of identical segments (i.e. one wavelength) is repeated and stretches to infinity in both directions ($+x$ and $-x$). Each segment is loaded identically and made up of a series of identical elements. In the case illustrated the elements are real, but quite generally the idea will be applicable to continual discretized in a series of identical element in each segment.

Isolating a typical segment between section **AA** and **BB** (Figure 2), the finite element formulations given in the previous section is used for the analysis. As all segments are identical, a simple reasoning shows that

$$\begin{aligned} &p(x = AA, z; t) = p(x = BB, z; t), \quad u(x = AA, z; t) = u(x = BB, z; t) \\ &w(x = AA, z; t) = w(x = BB, z; t), \quad \text{etc.} \end{aligned} \tag{26}$$

This concept has been first used by Zienkiewicz and Scott[47] in analysis of turbine and pump impellers. Since the present boundary value problem is a type of periodical loading, it is

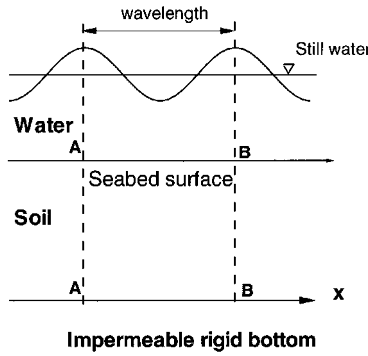

Figure 2. Principle of repeatability

convenient to employ this concept in the problem of wave–seabed interaction to obtain the solution without pipeline.

3.3. Numerical procedure

Since the analytical solutions for the wave-induced soil response in Gibson soil have not been available until now, the first step to solve the water–soil–pipe interaction in Gibson soil is to obtain the lateral boundary conditions.

To obtain the lateral boundary conditions, the wave–seabed interaction can be solved by employing the principle of repeatability. Once the later boundary conditions are obtained, the whole wave–seabed–pipe problem with pipeline can be solved. Since the local refinement of the Finite-Element (FE) mesh always has to be taken into account in the region near a structure, because a concentration of stresses is to be expected. To improve the accuracy of the solution in this region, we use two different mesh systems. As seen in Figure 3, a four-node iso-parameteric element is used in the region near the pipeline, $|r| \leqslant 2R$. Outside this region, a four-nodal rectangular element is used. This kind of mesh has been used for treating the problem around a pipe-like structure.[44] In this study, a mesh with 875 nodes and 806 elements is used for numerical calculations. After some preliminary study, this mesh is sufficient for the numerical examples presented here.

4. NUMERICAL RESULTS AND DISCUSSIONS

Based on the finite element model presented previously, some numerical examples are presented in this section. In a natural marine sedimentary seabed, the soil shear modulus usually increases with soil depth.[19,20] For variable shear modulus (see Figure 4), Type G_1 is for $G(z) = G_o = G_b$ ($=$ constant, G_o represents the shear modulus at the seabed surface and G_b is the shear modulus at the impermeable bottom), which is the conventional assumption of constant shear modulus. Types G_2 and G_3, $G(z) = G_o[1 + \alpha_1(z/h - 1)]$ is for a linear increase in shear modulus with burial depth. Type G_4, $G_4(z) = G_o e^{\alpha_1(z/h-1)}$, is for an exponential increase in shear modulus with depth. It is noted that types G_2 and G_3 have same depth function with different slopes, but type G_3 and

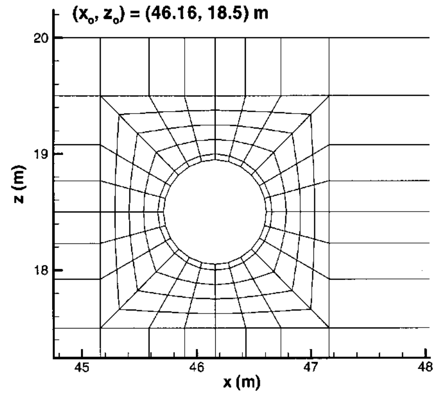

Figure 3. Sketch of the Finite-Element mesh discretization in the vicinity of buried submarine pipeline

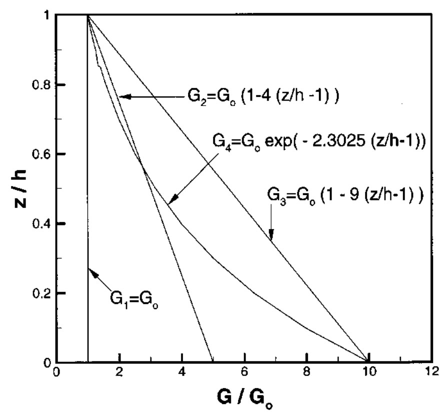

Figure 4. Four different function are examined for soil matrix with variable shear modulus in the present study

G_4 have same values of G_o and G_b with different depth functions. Two different soils (Soils A and B) are considered as examples here. The wave and soil characteristics are tabulated in Table I.

Since the major objective of this paper is to investigate the wave-induced pore pressure around a pipe in a Gibson soil, we only discussed the effects of variable shear modulus, geometry of the pipe and the degree of saturation on the wave-induced pore pressure herein. For the effects of other soil parameters and wave characteristics on the soil response, readers can refer to the first author's previous works for the case without pipeline.[10,31,32,34,36,37]

4.1. *Verification and comparisons*

Since previous investigations for the wave-induced soil response in Gibson soil around a buried pipeline have not been available until now, one of the possible verifications of the present model is

Table I. Input data for case study

Wave characteristics	
Wave period T	10·0 s
Water depth d	10·0 m
Wavelength L	92·32 m
Soil characteristics	
Thickness of seabed h	20 m
Poisson's ratio μ	0·3333
Porosity n'	0·4
Shear modulus G_o	5×10^6 N/m^2
The degree of saturation S	0·95–1·0
Permeability K	10^{-2} m/s (Soil A)
	10^{-4} m/s (Soil B)
Pipe characteristics	
Centre of the pipe (x_o, z_o)	$(L/2, h-b) = (46{\cdot}16, h-b)$
Radius R	0·5–1·0 m
Burial depth b	1·5–2·5 m

to reduce to its special case: a uniform seabed without pipeline.[36] Figure 5 illustrates the distribution of the wave-induced pore pressure (p/p_o) versus wave phase $(kx - \omega t)$ in a saturated seabed with uniform shear modulus. In the figure, the solid lines represent the results from the present model and the dotted lines are for previous analytical solution.[36] The comparison shows a fairly good agreement between two solutions.

Based on the same input data, a comparison between the wave-induced pore pressure without the pipe (in dashed lines) and with the pipe (in solid lines) is presented in Figure 6. The radius of the pipe $R = 0.5$ m and burial depth $b = 1{\cdot}5$ m are used in this example. It is observed that the influence of the existing pipe on the wave-induced pore pressure is significant in the region near the pipeline. However, this influence will become insignificant and vanish far away from the pipe.

4.2. Effect of variable shear modulus

Shear modulus of the soil is defined as the proportional coefficient in the shear stress–shear strain relationship. It has been reported that shear modulus of the seabed significantly affects the wave-induced soil response, especially in a seabed of finite thickness.[36] In the field, the shear modulus of the seabed increases as the soil depth increases.[19,20] Gibson soil is one of the examples that have been studied in consolidation problem.[18] In this section, the influences of variable shear modulus on the wave-induced pore pressure around a pipeline will be investigated.

Contours of the wave-induced pore pressure in the vicinity of the pipeline with uniform (G_1) and variable shear modulus (G_3) are presented in Figure 7(a). In the figure, the dashed lines represent the results of uniform shear modulus, while solid lines represent the results of variable shear modulus. As seen in Figure 7(a), the amplitude of the pore pressure with variable shear modulus is greater than that with uniform permeability when $z \leqslant h - b$. However, the results will reverse when $h - b \leqslant z \leqslant h$, except near the surface of the pipe.

Figure 7(b) shows the distributions of the wave-induced pore pressure along the surface of the pipe in Soil A. The pore pressures on the upper half surface of the pipe (i.e. $0 \leqslant \theta \leqslant \pi$, θ is defined

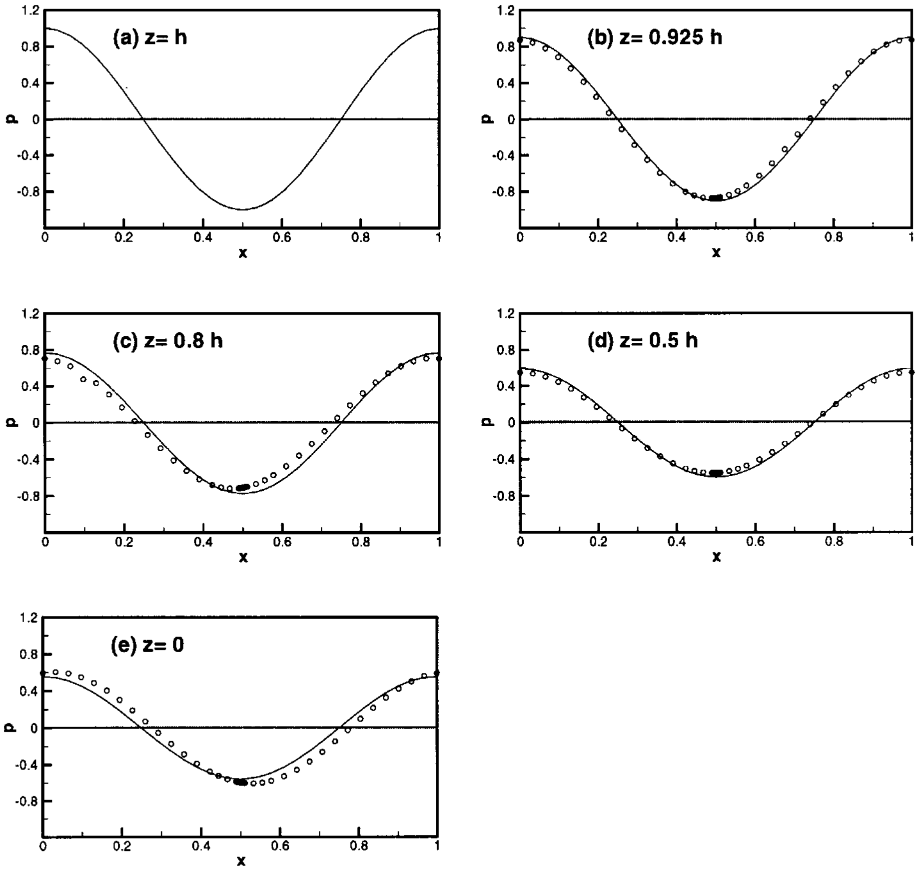

Figure 5. Comparison of pore pressure between analytical solution[36] (in circle '○') and the present model (in solid line)

in Figure 1) are almost unaffected by variable shear modulus G_i. However, the influence of variable shear modulus becomes somewhat significant on the lower half surface (i.e. $\pi \leqslant \theta \leqslant 2\pi$). It is noted that the results of G_1 and G_2 are almost identical to each other (the difference is hard to see in the graph). It is also found that the results of pore pressure with G_3 and G_4, which have different depth function with same values of G_b and G_o, are somewhat different. This implies that the distribution of shear modulus also affects the wave-induced soil response.

Similarly, Figure 7(c) illustrates the pore pressure around the pipeline in Soil B. The figure clearly shows that the influence of variable shear modulus on the pore pressure becomes more significant in Soil B (with low permeability). It is noted that the amplitude of pore pressure decreases as G_b/G_o increases with same types of depth function. For example, G_2 and G_3. However, with different types of depth function, the pore pressure will be changed even though they have same values of G_b/G_o . For example, G_3 and G_4 in Figure 7(c). It is also noted that the pore pressure on the surface of the pipe in Soil A is about three times of that in Soil B.

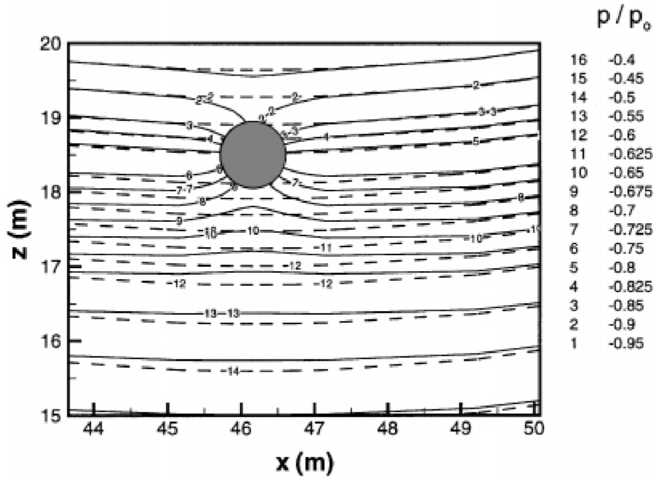

Figure 6. Contours of the wave-induced pore pressure p/p_o (a) without a pipe (in dashed lines) and (b) with a pipe (in solid lines) in Soil A with uniform shear modulus (G_1). ($b = 1{\cdot}5$ m, $R = 0{\cdot}5$ m, $S = 0{\cdot}985$)

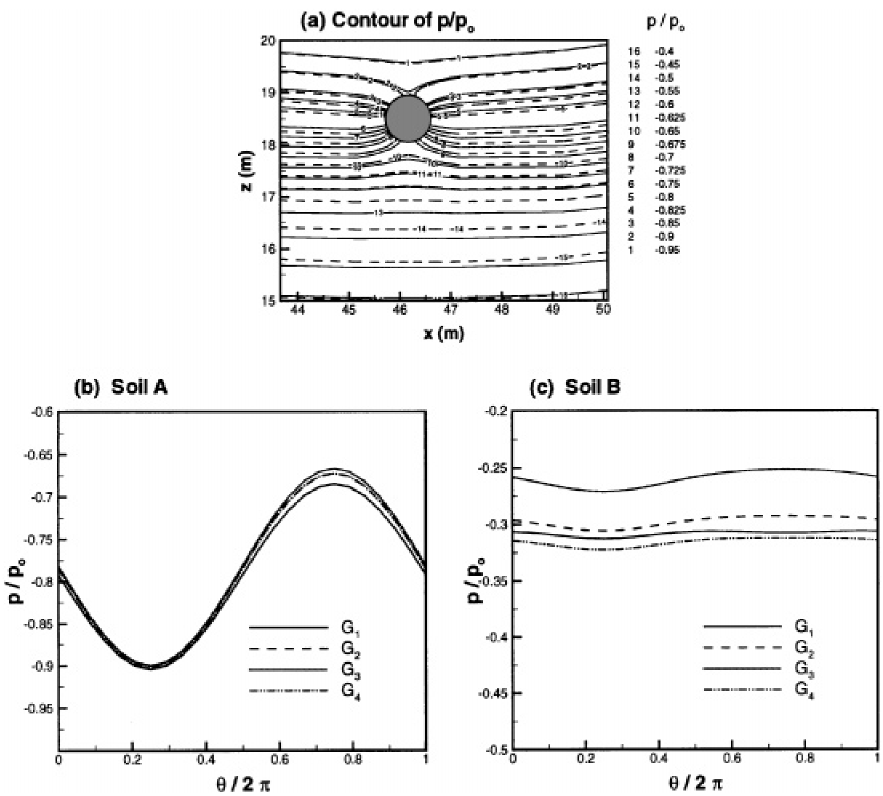

Figure 7. (a) Contours of the wave-induced pore pressure (dashed lines for G_1 and solid lines for G_3), and the pore pressure around the pipe in (b) Soil A and (c) Soil B. ($b = 1{\cdot}5$ m, $R = 0{\cdot}5$ m, $S = 0{\cdot}985$)

4.3. Effect of radius of the pipe

Besides variable shear modulus, radius of the pipe is another important factor that affects the distribution of the pore pressure. Figures 8(a)–(c) illustrate the contours of the normalized pore pressure ($|p|/p_o$) with different pipe radius ($R = 0{\cdot}5$, $0{\cdot}75$ and $1{\cdot}0$ m) in Soil A with variable shear modulus (G_3). The figures clearly show that the region affected by the existence of the pipeline becomes larger as R increases. This implies that the pipe radius affects the disturbed region of the pipeline.

The wave-induced pore pressures around the pipeline are presented in Figure 8(d). As seen in the figure, the amplitude pore pressure ($|p|/p_o$) on the upper half surface of the pipe ($0 \leqslant \theta \leqslant \pi$) decreases as R increases. However, $|p|/p_o$ increases R decreases on the lower half pipe ($\pi \leqslant \theta \leqslant 2\pi$). This implies that the radius of the pipe directly affects the distribution of the pore water pressure on the surface of the pipeline. Therefore, the existence of the pipe may enhance the potential of the wave-induced seabed instability (such as liquefaction and shear failure). However, the pore pressures at $\theta = 0$, π, 2π are constant for different pipe radius [Figure 8(d)].

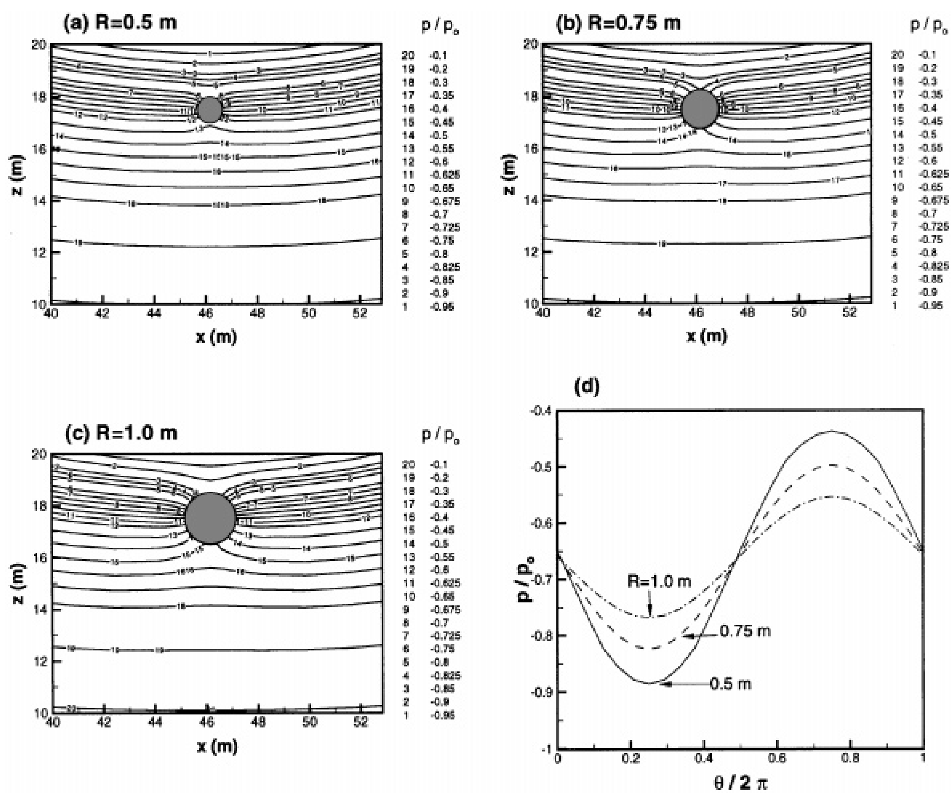

Figure 8. Contours of the wave-induced pore pressure p/p_o with different radius (a) $R = 0{\cdot}5$ m, (b) $R = 0{\cdot}75$ m, (c) $R = 1{\cdot}0$ m, and (d) the pore pressure around the pipe in Soil A with variable shear modulus (G_3). ($b = 2{\cdot}5$ m, $S = 0{\cdot}985$)

4.4. *Effect of burial depth*

The burial depth of the pipe is another important factor in the design of pipeline. Three burial depths, $b = 1{\cdot}0$, $1{\cdot}5$ and $2{\cdot}0$ m, are considered as examples here. The radius of the pipe is taken as $0{\cdot}5$ m. As seen in Figures 9(a)–(c), the region that is affected by the existence of the pipe moves up or down with the burial depth, without changing the size of the affected region. The amplitude of wave-induced pore pressures ($|p|/p_o$) on the pipe surface increases as burial depth (b) decreases. This implies that pore pressure on the pipe surface becomes larger when the pipeline is buried near the surface of the seabed. Since the wave-induced seabed instability always occurs near the seabed surface, the existence of the pipeline may enhance the potential of the wave-induced seabed instability.

4.5. *Effect of the degree of saturation*

It has been well known that the degree of saturation dominates the wave-induced oscillatory soil response.[7,34,48] It is commonly to found gas within the marine sediment, implying

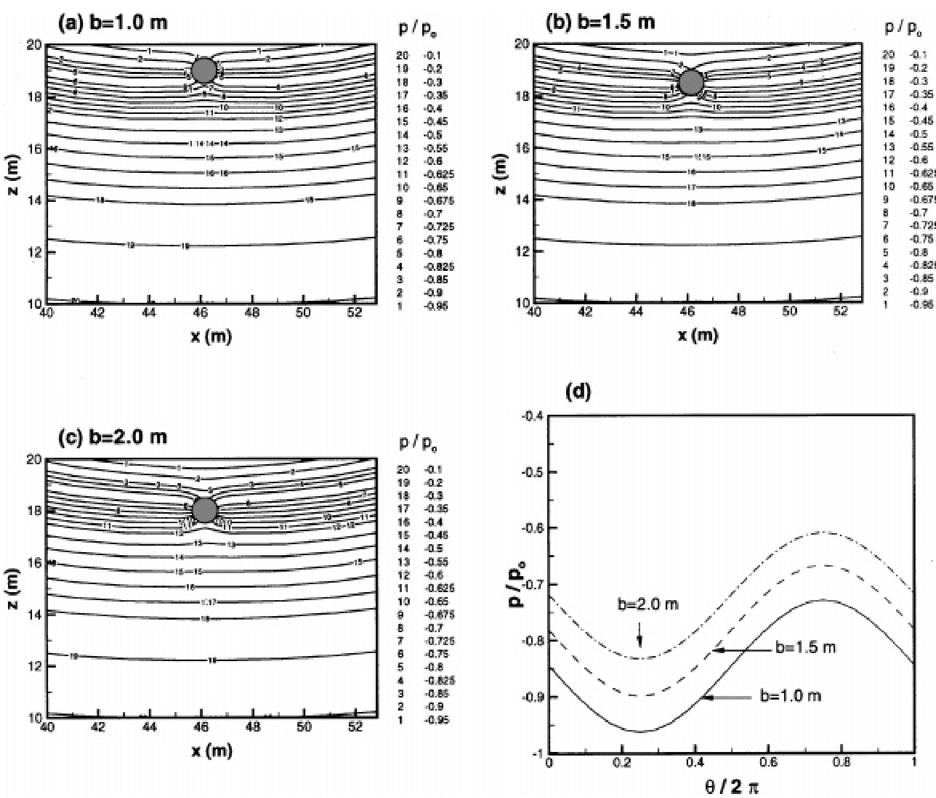

Figure 9. Contours of the wave-induced pore pressure p/p_o with different burial depth (a) $b = 1{\cdot}0$ m, (b) $b = 1{\cdot}5$ m, (c) $b = 2{\cdot}0$ m, and (d) the pore pressure around the pipe in Soil A with variable shear modulus (G_3). ($R = 0{\cdot}5$ m, $S = 0{\cdot}985$)

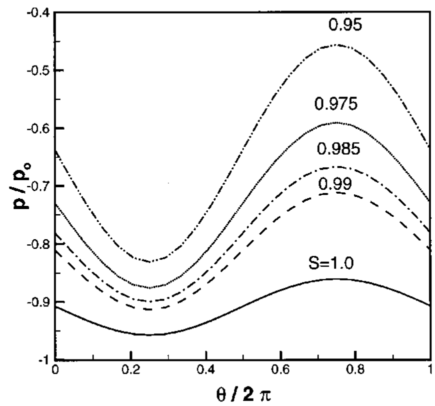

Figure 10. Wave-induced pore pressure around the pipe with various degrees of saturation S in Soil A with variable shear modulus (G_3). ($b = 1{\cdot}5$ m, $R = 0{\cdot}5$m)

unsaturated condition.[49] Figure 10 illustrates the effects of the degree of saturation (S) on the wave-induced pore water pressure on the surface of the pipeline. It is observed that amplitude of pore pressure decreases as S decreases. It is also found that the soil response is very sensitive to the degree of saturation, especially near saturated condition. For example, a great difference between $S = 1{\cdot}0$ and $0{\cdot}99$.

4.6. Further applications of the parametric study

Based on the above parametric study, the following applications could be carried out with more sophisticated investigations in the future:

Wave-induced seabed instability: Since the wave-induced pore pressure is the key factor in the evaluation of the wave-induced seabed instability (such as shear failure and liquefaction), some tentatively ideas can be found from the previous parametric study. Because the wave-induced seabed instability may only occur near the seabed surface, it is expected that a larger pipe buried near the seabed surface will enhance the potential of the wave-induced seabed instability. However, the detail of the wave-induced seabed instability requires more sophisticated investigations in the future.

Stress distribution within the pipe: The distribution of stresses within the pipe itself is another important factor in the design procedure of pipeline. The distribution of the wave-induced pore pressure along the pipeline will directly affect the deformation of the pipe. A larger pore pressure acting on the pipe may enhance the occurring potential of the crack of the pipe. For example, a small radius pipe may under the action of a larger wave-induced pore pressure on the lower half of the pipe, but a larger pipe may enhance the pore pressure on the upper half of the pipe.

5. CONCLUSIONS

This paper is aimed at investigating the influences of variable shear modulus on the wave-induced pore pressure in the vicinity of a buried pipeline. A finite element model has been proposed for the

wave–seabed–pipe interaction problem in Gibson soil. The following conclusions may be drawn:

(1) A comprehensive verification of the present model without a pipe against the previous analytical solution has been performed, through its reduction to the special case of uniform shear modulus.
(2) Variable shear modulus significantly affects the pore pressure, especially in Soil B with low permeability. Thus, variable shear modulus must be considered in analysis for a finer material.
(3) The pipe radius (R) directly affects the distribution of the pore pressure on the upper and lower half pipe. The pipe radius also affects, as well as the size of region that is affected by the existence of the pipeline.
(4) Although burial depth (b) does not affect on the disturbed region of the pipeline, it affects the location of the disturbed region. Thus, it also affects the amplitude of pore pressure on the pipe surface. When the pipe is buried near the surface of the seabed, the pore pressure on the pipe surface becomes larger. Therefore, in summary, the burial depth and pipe radius a larger pipe buried near the seabed surface will enhance the potential of the wave-induced seabed instability.

In this paper, only the results of wave-induced pore pressure in the vicinity of a buried pipeline in Gibson soil have been presented. However, the capability of the proposed model is by no means limited to this type of problem. Problems of multiple pipelines, structures other than pipelines, three-dimensional structures and so on can also be investigated. Also, the solution gives information not only the pore pressure, but also on the soil displacements and effective stresses that can be used to analyse seabed instability for engineering practice. Some those aspects are currently being investigated by the first author.

ACKNOWLEDGMENTS

The work described here is part of the activities of Special Research Centre for Offshore Foundation Systems at The University of Western Australia, established and supported under Australian Research Council's Research Centres Program. Part of this work is also supported by National Science Council in Taiwan. Reviewers' helpful comments are also appreciated.

APPENDIX: LIST OF COEFFICIENT MATRIX

The coefficient matrices $\mathbf{B}_i$ ($i = 1$–6) in equations (19) and (23) are listed as follows:

$$\mathbf{B}_i = [b_{i1} \;\; b_{i2} \ldots b_{in_e}] \tag{27}$$

$$b_{i1} = \begin{bmatrix} \dfrac{\partial N_i}{\partial x} & 0 \\ 0 & \dfrac{\partial N_i}{\partial x} \\ \dfrac{\partial N_i}{\partial z} & 0 \\ 0 & \dfrac{\partial N_i}{\partial z} \end{bmatrix} \tag{28}$$

$$b_{2i} = \begin{bmatrix} N_i & 0 \\ 0 & N_i \end{bmatrix} \tag{29}$$

$$b_{3i} = b_{1i}^{\mathrm{T}} \tag{30}$$

$$b_{i4} = \begin{bmatrix} \frac{\partial N_i}{\partial x} & 0 & 0 & 0 \\ 0 & \frac{\partial N_i}{\partial x} & 0 & 0 \\ 0 & 0 & \frac{\partial N_i}{\partial z} & 0 \\ 0 & 0 & 0 & \frac{\partial N_i}{\partial z} \\ \frac{\partial N_i}{\partial z} & 0 & \frac{\partial N_i}{\partial x} & 0 \\ 0 & \frac{\partial N_i}{\partial z} & 0 & \frac{\partial N_i}{\partial x} \end{bmatrix} \tag{31}$$

$$b_{5i} = \begin{bmatrix} N_i & 0 & 0 & 0 \\ 0 & N_i & 0 & 0 \\ 0 & 0 & N_i & 0 \\ 0 & 0 & 0 & N_i \end{bmatrix} \tag{32}$$

The coefficient matrix $\mathbf{D}_i$ in equation (19) and (23) are given

$$\mathbf{D}_1 = \begin{bmatrix} \frac{\gamma_w}{K} & 0 & 0 & 0 \\ 0 & \frac{\gamma_w}{K} & 0 & 0 \\ 0 & 0 & \frac{\gamma_w}{K} & 0 \\ 0 & 0 & 0 & \frac{\gamma_w}{K} \end{bmatrix} \tag{33}$$

$$\mathbf{D}_2 = \begin{bmatrix} 0 & -n'\beta\omega \\ n'\beta\omega & 0 \end{bmatrix} \tag{34}$$

$$\mathbf{D}_3 = \begin{bmatrix} 0 & \omega \\ -\omega & 0 \end{bmatrix} \tag{35}$$

$$\mathbf{D}_4 = \frac{2G}{1-2\mu}\begin{bmatrix} 1-\mu & 0 & \mu & 0 & 0 & 0 & \\ 0 & 1-\mu & 0 & \mu & 0 & 0 & \\ \mu & 0 & 1-\mu & 0 & 0 & 0 & \\ 0 & \mu & 0 & 1-\mu & 0 & 0 & \\ 0 & 0 & 0 & 0 & 0 & \frac{1-2\mu}{2} & 0 \\ 0 & 0 & 0 & 0 & 0 & 0 & \frac{1-2\mu}{2} \end{bmatrix} \tag{36}$$

REFERENCES

1. R. Silvester and J. R. C. Hsu, 'Sines revisited', *J. Waterways Port Coastal Ocean Engng. ASCE*, **115**(3), 327–344 (1989).
2. H. Lundgren, J. H. C. Lindhardt and C. J. Romhild, 'Stability of breakwaters on porous foundation', *Proc. 12th Int. Conf. Soil Mechanics and Foundation Engineering*, London, 1989, pp. 451–454.
3. E. C. Clukey, J. A. Vermersch, S. P. Koch and W. C. Lamb, 'Natural densification by wave action of sand surrounding a buried offshore pipeline', *Proc. 21st Annual Offshore Technology Conf.*, Houston, Texas, 1989, pp. 291–300.
4. T. Yamamoto and T. Torii, 'Seabed shear modulus profile inversion using surface gravity (water) wave-induced bottom motion', *Geophys. J. Roy. Soc.*, **85,** 413–431 (1986).
5. T. Nye and T. Yamamoto, 'Field test of buried ocean-wave directional spectrometer system', *J. Waterway Port, Coastal Ocean Engng. ASCE* **120**(5), 451–466 (1994).
6. T. Yamamoto and A. Turgut, 'Acoustic wave propagation through porous media with arbitrary pore size distributions', *J. Acoust. Soc. Am.*, **83**(5), 1744–1751 (1988).
7. F. B. J. Barends and S. E. J. Spierenburg, 'Interaction between ocean waves and sea-bed', *Proc. Int. Conf. on Geotechnical Engineering for Coastal Development-Theory and Practice on Soft Ground* (*Geot-Coastal'91*), Yokohama, Japan, 1991, pp. 1091–1108.
8. M. S. Rahman, 'Wave-induced instability of seabed: mechanism and conditions', *Mar. Geotechnol.* **10,** 277–299 (1991).
9. M. S. Rahman, 'Instability and movement of oceanfloor sediments: a review', *Int. J. Offshore Polar Engng.*, **7**(3), 220–225 (1997).
10. D. S. Jeng, 'Wave-induced seabed instability in front of a breakwater', *Ocean Engng.* **24**(10), 887–917 (1997).
11. H. Nago, S. Maeno, T. Matsumoto and Y. Hachiman, 'Liquefaction and densification of loosely deposited sand bed under water pressure variation', *Proc. 3rd (1993) Int. Offshore and Polar Engineering Conf.,* Singapore, 1993, pp. 578–584.
12. K. Zen and H. Yamazaki, 'Mechanism of wave-induced liquefaction and densification in seabed', *Soil Found.*, **30**(4), 90–104 (1990).
13. T. Yamamoto, H. L. Koning, H. Sellmejjer and E. V. van Hijum, 'On the response of a poro-elastic bed to water waves', *J. Fluid Mech.*, **87**(2), 193–206 (1978).
14. O. S. Madsen, 'Wave-induced pore pressures and effective stresses in a porous bed', *Géotechnique*, **28**(4), 377–393 (1978).
15. H. B. Seed and M. S. Rahman, 'Wave-induced pore pressure in relation to ocean floor stability of cohesionless soils', *Mar. Geotechnol.*, **3**(2), 123–150 (1978).
16. F. B. J. Barends and P. A. Ruygrok, 'The cyclic liquefaction potential of a submerged cohesionless sand bed: a practical method', *Proc. 8th Int. Conf. on Behavior of Offshore Structures* (*BOSS'97*), Vol. 1, Delft, 1997, pp. 71–84.
17. A. Verrujit, M. P. J. de Bruijn and B. Muralidhar, 'Liquefaction around buried pipelines', *Proc. 8th Int. Conf. on Behavior of Offshore Structures* (*BOSS'97*), Vol. 1, Delft, 1997, pp. 99–107.
18. R. E. Gibson, 'Some results concerning displacements and stresses in a non-homogeneous elastic half-space', *Géotechnique*, **17,** 58–67 (1967).
19. M. Badiey, K. Zen, H. Yamazaki and H. Suzuki, 'Field and laboratory measurement of shear modulus profile in seabed', *Rep. Port Harbour Res. Inst. Jpn.*, **29**(4), 3–26 (1990).
20. H. Suzuki, K. Ando, M. Kitahara, M. Badiey and T. Yamamoto, 'Shear modulus profile measurement of the shallow-water seabed in japan', *Proc. Int. Conf. on Geotechnical Engineering for Coastal Development-Theory and practice on soft ground* (*Geot-Coastal'91*), Vol. 1, Yokohama, Japan, 1991, pp. 99–104.
21. T. Yamamoto, 'Wave induced instability seabeds', *Proc. A.S.C.E. Spec. Conf.: Coastal Sediments'77*, Charleston, SC, 1977, pp. 898–913.
22. T. Yamamoto, 'Wave-induced pore pressures and effective stresses in inhomogeneous seabed foundations', *Ocean Engng.*, **8,** 1–16 (1981).

23. C. C. Mei and M. A. Foda, 'Wave-induced response in a fluid-filled poro-elastic solid with a free surface-a boundary layer theory', *Geophys. J. Roy. Astron. Soc.*, **66,** 597–631 (1981).
24. J. R. C. Hsu and D. S. Jeng, 'Wave-induced soil response in an unsaturated anisotropic seabed of finite thickness', *Int. J. Numer. Anal. Meth. Geomech.*, **18**(11)**,** 785–807 (1994).
25. D. S. Jeng and B. R. Seymour, 'Wave-induced pore pressure and effective stresses in a porous seabed with variable permeability', *J. Offshore Mech. Arctic Engng.*, *ASME* **119**(4)**,** 226–233 (1997).
26. W. Magda, 'Study on one-dimensional model for wave-induced pore wave pressure', *Proc. IVth Russian Conf. with Foreign Participation*, 1993, pp. 179–191.
27. B. Gatmiri, 'A simplified finite element analysis of wave-induced effective stress and pore pressures in permeable sea beds', *Géotechnique*, **40**(1)**,** 15–30 (1990).
28. B. Gatmiri, 'Response of cross-anisotropic seabed to ocean waves', *J. Geotech. Engng.*, *ASCE* **118**(9)**,** 1295–1314 (1992).
29. S. D. Thomas, 'A finite element model for the analysis of wave induced stresses, displacements and pore pressures in an unsaturated seabed. I: theory', *Comput. Geotech.*, **8**(1)**,** 1–38 (1989).
30. S. D. Thomas, 'A finite element model for the analysis of wave induced stresses, displacements and pore pressures in an unsaturated seabed. II: model verification', *Comput. Geotech.*, **17**(1)**,** 107–132 (1995).
31. Y. S. Lin and D. S. Jeng, 'The effect of variable permeability on the wave-induced seabed response', *Ocean Engng.*, **124**(7)**,** 623–643 (1997).
32. D. S. Jeng and Y. S. Lin, 'Wave-induced pore pressure in a cross-anisotropic seabed with variable soil characteristics', *The 8th* (*1998*) *Int. Offshore and Polar Engineering Conf.* (*ISOPE98*), Vol. 1, Montréal, Canada, 1998, pp. 598–604.
33. W. Raman-Nair and G. C. W. Sabin, 'Wave-induced failure of poro-plastic seabed slopes: a boundary element study', *Proc. Inst. Civil Engrs UK*, *Part 2*, **91,** 771–794 (1991).
34. J. R. C. Hsu, D. S. Jeng and C. P. Tsai, 'Short-crested wave-induced soil response in a porous seabed of infinite thickness', *Int. J. Numer. Anal. Meth. Geomech.*, **17**(8)**,** 553–576 (1993).
35. D. S. Jeng, 'Soil response in cross-anisotropic seabed due to standing waves', *J. Geotech. Geoenviron. Engng.*, *ASCE* **123**(1)**,** 9–19 (1997).
36. D. S. Jeng and J. R. C. Hsu, 'Wave-induced soil response in a nearly saturated sea-bed of finite thickness', *Géotechnique*, **46**(3)**,** 427– 440 (1996).
37. D. S. Jeng and B. R. Seymour, 'Response in seabed of finite depth with variable permeability', *J. Geotech. Geoenviron. Engng.*, *ASCE*, **123**(10)**,** 902–911 (1997).
38. H. MacPherson, 'Wave forces on pipelines buried in permeable seabed', *J. Waterway Port Coastal Ocean Div.*, *ASCE* **104**(4)**,** 407–419 (1978).
39. W. G. MacDougal, S. H. Davidson, P. L. Monkmeyer and C. K. Sollitt, 'Wave-induced forces on buried pipelines', *J. Waterway Port Coastal Ocean Engng.*, *ASCE* **114**(2)**,** 220–236 (1988).
40. S. E. J. Spierenburg, 'Wave-induced pore pressures around submarine pipelines', *Coastal Engng.*, **10,** 33–48 (1986).
41. M. A. Biot, 'General theory of three-dimensional consolidation', *J. Appl.*, *Phys.*, **12**(2)**,** 155–164 (1941).
42. A. Verruijt, 'Elastic storage of aquifers', in R. J. M. De Wiest (ed.), *Flow Through Porous Media*, Chapter, Academic Press, New York, 1969, pp. 331–376.
43. A. H. D. Cheng and P. L. F. Liu, 'Seepage force on a pipeline buried a poroelastic seabed under wave loading', *Appl. Ocean Res.*, **8**(1)**,** 22–32 (1986).
44. W. Magda, 'Wave-induced uplift force acting on a submarine buried pipeline: finite element formulation and verification of computations', *Comput. Geotech.*, **19**(1)**,** 47–53 (1996).
45. W. Magda, 'Wave-induced uplift force acting on a submarine buried pipeline in a compressible seabed', *Ocean Engng.*, **24**(6)**,** 511–576 (1997).
46. O. C. Zienkiewicz and R. L. Taylor, *The Finite Element Method*, McGraw-Hill, New York, 1989.
47. O. C. Zienkiewicz and F. C. Scott, 'On the principle of repeatability and its application in analysis of turbine and pump impellers', *Int. J. Numer. Meth. Engng.*, **9,** 445–452 (1972).
48. S. Pietruszczak and G. N. Pande, 'Constitutive relations for partially saturated soils containing gas inclusions', *J. Geotech. Engng.*, *ASCE*, **122**(1)**,** 50–59 (1996).
49. M. I. Esrig and R. C. Kirby, 'Implication of gas content for predicting the stability of submarine slopes', *Mar. Geotechnol.* **2**(2)**,** 81–100 (1977).

